Electronic Supplementary Information

Formation of Charge-Transfer Complexes in Ionic Crystals Composed of 1,3-Bis(dicyanomethylidene)indan Anion and Viologens Bearing Alkyl Chains

Erika Saito, Ryohei Yamakado*, Taichi Yasuhara, Hiroto Yamaguchi, Shuji Okada and Tsukasa Yoshida*

Department of Organic Materials Science, Graduate School of Organic Materials Science, Yamagata University, Yonezawa 992-8510, Japan, Fax: +81 238 26 3741; Tel: +81 238 26 3088; E-mail: yamakado@yz.yamagata-u.ac.jp

Table of Contents

1. Synthetic procedures and spectroscopic data

General procedures. Starting materials were purchased from Kanto Chemical, TCI, and Sigma-Aldrich, and used without further purification unless otherwise stated. ^{1}H and ^{13}C nuclear magnetic resonance (NMR) spectroscopies were investigated on JEOL ECX-500 500 MHz and ECZ-600 600 MHz spectrometers using DMSO-d_6 (δ 2.50 and 39.5 for ^{1}H and ^{13}C NMR, respectively) as the internal standards. Ultraviolet (UV)-visible (Vis)-near infrared (NIR) diffuse reflectance spectra were recorded on a JASCO V-750 spectrometer using a 10 mm quartz cell. UV−vis−NIR diffuse reflectance spectra were recorded on a JASCO V-670 spectrometer using powdered samples. Samples were supported on filter paper, which was also used to provide the background reference.

Typical procedure of the synthesis of 1,1'-dialkyl-4,4'-bipyridinium dihalide (Cn^{2+}-2X^{-}). 4,4'-Bipyridine (1.56 g, 10 mmol) was added to 3 equivalents of alkylhalide (30 mmol) in acetonitrile (20 mL). The mixture was heated at 65 °C to complete dissolution and stirred 48 h. The precipitate in the reaction mixture was filtered and washed with THF. The compound was recrystallized from MeOH.

1,1'-Dipropyl-4,4'-bipyridinium dibromide (C3^{2+}-2Br^{-}). Yellow powder, Yield: 62%, M.p.: 287°C. ^{1}H NMR (600 MHz, DMSO-d_6, δ): 0.89 (6H, t, J = 7.2 Hz), 1.99 (4H, td, J = 7.2 Hz), 4.75 (4H, t, J = 7.2 Hz), 8.88 (4H, d, J = 6.9 Hz), 9.52 (4H, d, J = 6.9 Hz). ^{13}C NMR (126 MHz, DMSO-d_6, δ): 10.11, 24.11, 61.98, 126.60, 145.64, 148.56.

1,1'-Dibutyl-4,4'-bipyridinium dibromide (C4^{2+}-2Br^{-}). Yellow powder, Yield: 61%, M.p.: 284°C. ^{1}H NMR (400 MHz, DMSO-d_6, δ): 0.94 (6H, t, J = 7.4 Hz), 1.33 (4H, td, J = 7.4 Hz), 1.93—2.00 (4H, m), 4.70 (4H, t, J = 7.2 Hz), 8.79 (4H, d, J = 6.7 Hz), 9.40 (4H, d, J = 6.7 Hz). ^{13}C NMR (126 MHz, DMSO-d_6, δ): 13.23, 18.70, 32.60, 60.65, 126.63, 145.67, 148.64.

1,1'-Dipentyl-4,4'-bipyridinium dibromide (C5^{2+}-2Br^{-}). Yellow powder, Yield: 62%, M.p.: 274°C. ^{1}H NMR (500 MHz, DMSO-d_6, δ): 0.88 (6H, t, J = 6.8 Hz), 1.29—1.37 (8H, m), 1.97—2.02 (4H, m), 4.74 (4H, t, J = 7.8 Hz), 8.82 (4H, d, J = 6.5 Hz), 9.45 (4H, d, J = 6.5 Hz). ^{13}C NMR (126 MHz, DMSO-d_6, δ): 13.83, 21.65, 27.57, 30.54, 60.84, 126.72, 145.80, 148.64.

1,1'-Dihexyl-4,4'-bipyridinium diiodide (C6^{2+}-2I^{-}). Orange red powder, Yield: 60%, M.p.: 279°C. ^{1}H NMR (500 MHz, DMSO-d_6, δ): 0.84—0.89 (6H, m), 1.27—1.37 (12H, m), 1.93—2.04 (4H, m), 4.698 (4H, t, J = 7.5 Hz), 8.77 (4H, d, J = 6.8 Hz), 9.37 (4H, d, J = 6.8 Hz). ^{13}C NMR (126 MHz, DMSO-d_6, δ): 13.73, 21.76, 25.00, 30.48, 60.94, 126.62, 145.62, 148.64.

Typical procedure of the synthesis of 1,1'-dialkyl-4,4'-bipyridinium 1,3-bis(dicyanomethilidene)indan (Cn^{2+}-2CMI^{-}). To an aqueous solution (1 mM) of 1,3-bis(dicyanomethylidene)indan (60.55 mg, 0.25 mmol), 2.51 mM NaOH aq (pH = 12.4) was added dropwise to be basic condition (pH = 9.6–10.0). To this solution, aqueous solution (125 mL) of 1,1—dipropyl—4,4'-bipridinium dihalide (0.125 mmol) was added, and the mixture was stirred for 24 h at r.t,. After removing the solvents, the residue was recrystallized from ethanol to afford **Cn^{2+}-2CMI^{-}**.

1,1'-Dimetyl-4,4'-bipridinium 1,3-bis(dicyanomethilidene)indan (C1^{2+}-2CMI^{-}). Deep orange purple powder, Yield 42%, M.p.: 260 °C (decomposition), ^{1}H NMR (400 MHz, DMSO-d_6, δ): 4.43 (6H, s), 5.70 (2H, s), 7.41-7.44 (4H, m), 7.88-7.93 (4H, m), 8.74 (4H, d, J = 6.7 Hz), 9.27 (4H, d, J = 6.7 Hz). ^{13}C NMR (126 MHz, DMSO-d_6, δ): 47.91, 50.26, 102.70, 117.69, 117.80, 121.44, 125.92, 130.01, 137.78, 146.51, 148.08, 158.05.

1,1'-Dietyl-4,4'-bipridinium 1,3-bis(dicyanomethilidene)indan (C2^{2+}-2CMI^{-}). Dark green powder, Yield 42%, M.p.: 243 °C, ^{1}H NMR (500 MHz, DMSO-d_6, δ): 1.61 (6H, t, J = 7.0 Hz), 4.72 (4H, q, J = 7.3 Hz), 5.70 (2H, s), 7.41-7.43 (4H, m), 7.89-7.92 (4H, m), 8.75 (4H, d, J = 6.3 Hz), 9.37 (4H, d, J = 6.3 Hz). ^{13}C NMR (126 MHz, DMSO-d_6, δ): 16.36, 50.40, 56.61, 102.76, 117.85, 117.94, 121.60, 126.50, 130.18, 137.82, 145.62, 148.47, 158.16.

1,1'-Dipropyl-4,4'-bipyridinium 1,3-bis(dicyanomethylidene)indan (C3^{2+}-2CMI^{-}). Deep purple powder, Yield 40%, M.p.: 242 °C, ^{1}H NMR (500 MHz, DMSO-d_6, δ): 0.94 (6H, t, J = 7.5 Hz), 1.99-2.04 (4H, m) 4.66 (4H, t, J = 7.0 Hz), 5.70 (2H, s), 7.41-7.42 (4H, m), 7.90-7.91 (4H, m), 8.76 (4H,

d, J = 7.0 Hz), 9.35 (4H, d, J = 7.0 Hz). ^{13}C NMR (126 MHz, DMSO-d_6, δ): 10.08, 24.02, 50.24, 62.20, 102.65, 117.67, 117.79, 121.43, 126.47, 129.95, 137.77, 145.60, 148.57, 158.04.

1,1'-Dibutyl-4,4'-bipiridinium 1,3-bis(dicyanomethylidene)indan (C4^{2+}-2CMI^{-}). Deep purple powder, Yield 44%, M.p.: 236 °C, ^{1}H NMR (500 MHz, DMSO-d_6, δ): 0.94 (6H, t, J = 7.2 Hz), 1.30-1.36 (4H, m), 1.92-1.98 (4H, m), 4.68 (4H, t, J = 7.6 Hz), 5.70 (2H, s), 7.42-7.44 (4H, m), 7.90-7.92 (4H, m), 8.77 (4H, d, J = 7.0 Hz), 9.37 (4H, d, J = 7.0 Hz). ^{13}C NMR (100 MHz, DMSO-d_6, δ): 13.15, 18.66, 32.52, 50.25, 60.66, 102.64, 117.68, 117.78, 121.43, 126.49, 129.95, 137.78, 145.61, 148.53, 158.03.

1,1'-Dipentyl-4,4'-bipridinium 1,3-bis(dicyanomethilidene)indan (C5^{2+}-2CMI^{-}). Deep purple powder, Yield 40%, M.p.: 228 °C, ^{1}H NMR (400 MHz, DMSO-d_6, δ): 0.89 (6H, t, J = 7.0 Hz), 1.25-1.36 (8H, m), 1.93-2.03 (4H, m), 4.68 (4H, t, J = 7.6 Hz), 5.71 (2H, s), 7.40-7.44 (4H, m), 7.88-7.94 (4H, m), 8.77 (4H, d, J = 7.2 Hz), 9.37 (4H, d, 7.2 Hz). ^{13}C NMR (126 MHz, DMSO-d_6, δ): 13.78, 21.66, 27.63, 30.55, 50.47, 61.00, 102.82, 117.89, 117.98, 121.61, 126.50, 130.15, 137.86, 145.76, 148.51, 158.16.

1,1'-Dihexyl-4,4'-bipridinium 1,3-bis(dicyanomethilidene)indan (C6^{2+}-2CMI^{-}). Dark purple powder, Yield 39%, M.p.: 184 °C, ^{1}H NMR (400 MHz, DMSO-d_6, δ): 0.87 (6H, t, J = 7.0 Hz), 1.27-1.35 (12H, m), 1.93-2.02 (4H, m), 4.68 (4H, t, J = 7.2 Hz), 5.71 (2H, s), 7.39-7.45 (4H, m), 7.88-7.93 (4H, m), 8.76 (4H, d, J = 6.8 Hz), 9.37 (4H, d, J = 6.8 Hz). ^{13}C NMR (126 MHz, DMSO-d_6, δ): 13.74, 21.82, 25.29, 27.92, 30.89, 50.27, 60.92, 102.64, 117.70, 117.81, 121.45, 126.43, 130.03, 137.80, 145.60, 148.53, 158.07.

1,1'-Diheptyl-4,4'-bipridinium 1,3-bis(dicyanomethilidene)indan (C7^{2+}-22CMI^{-}). Black powder, Yield 40%, M.p.: 153 °C, ^{1}H NMR (500 MHz, DMSO-d_6, δ): 0.86 (6H, t, J = 7.0 Hz), 1.21-1.36 (16H, m), 1.96-2.08 (4H, m), 4.67 (4H, t, J = 7.5 Hz), 5.70 (2H, s), 7.41-7.43 (4H, m), 7.89-7.91 (4H, m), 8.77 (4H, d, J = 6.3 Hz), 9.37 (4H, d, J = 6.3 Hz). ^{13}C NMR (126 MHz, DMSO-d_6, δ): 13.93, 21.98, 25.40, 28.08, 30.77, 31.03, 50.39, 60.94, 102.74, 117.84, 117.93, 121.59, 126.58, 130.17, 137.83, 145.74, 148.57, 158.16.

1,1'-Dioctyl-4,4'-bipridinium 1,3-bis(dicyanomethilidene)indan (C8^{2+}-2CMI^{-}). Dark purple powder, Yield 39%, M.p.: 132 °C, ^{1}H NMR (500 MHz, DMSO-d_6, δ): 0.85 (6H, t, J = 7.0 Hz), 1.20-1.39 (22H, m), 1.92-2.02 (4H, m), 4.67 (4H, t, J = 7.3 Hz), 5.70 (2H, s), 7.39-7.44 (4H, m), 7.88-7.93 (4H, m), 8.75 (4H, d, J = 6.5 Hz), 9.35 (4H, d, J = 6.5 Hz). ^{13}C NMR (126 MHz, DMSO-d_6, δ): 13.75, 21.89, 25.33, 28.22, 28.32, 30.61, 31.00, 50.26, 60.91, 102.67, 117.68, 117.79, 121.43, 126.46, 129.94, 137.78, 145.59, 148.49, 158.04.

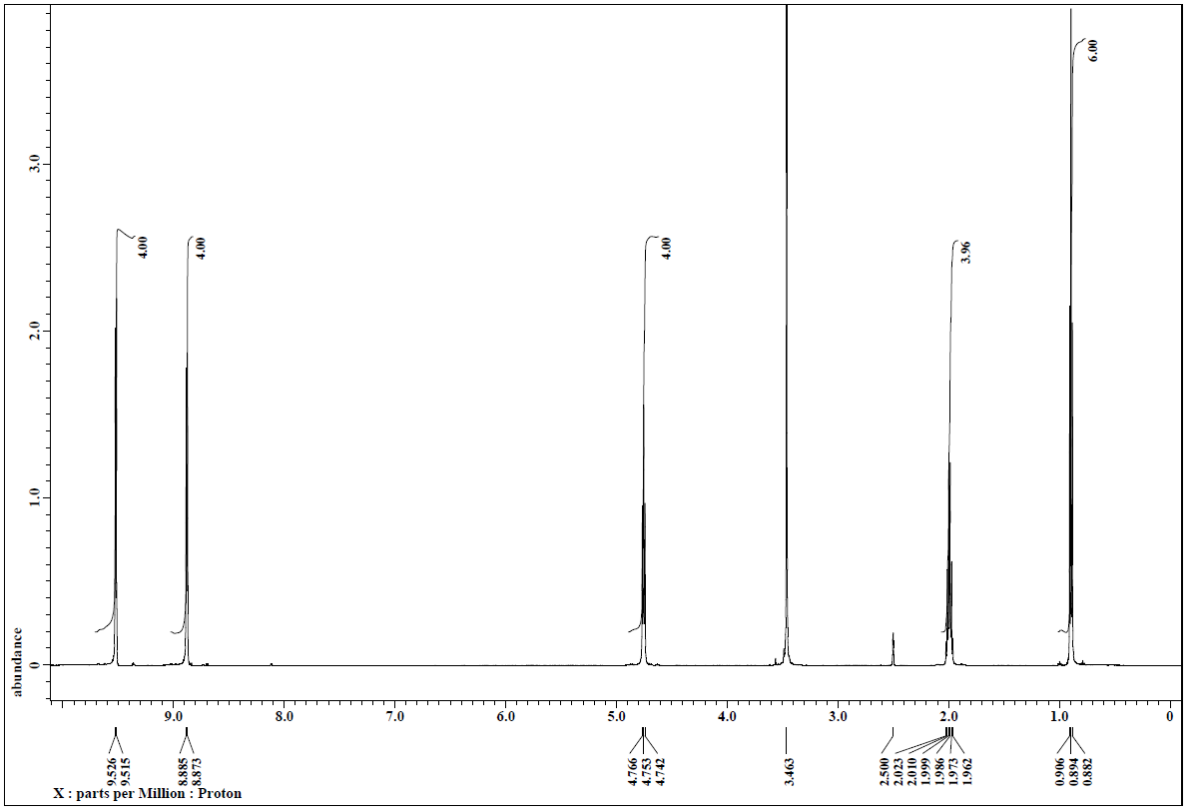

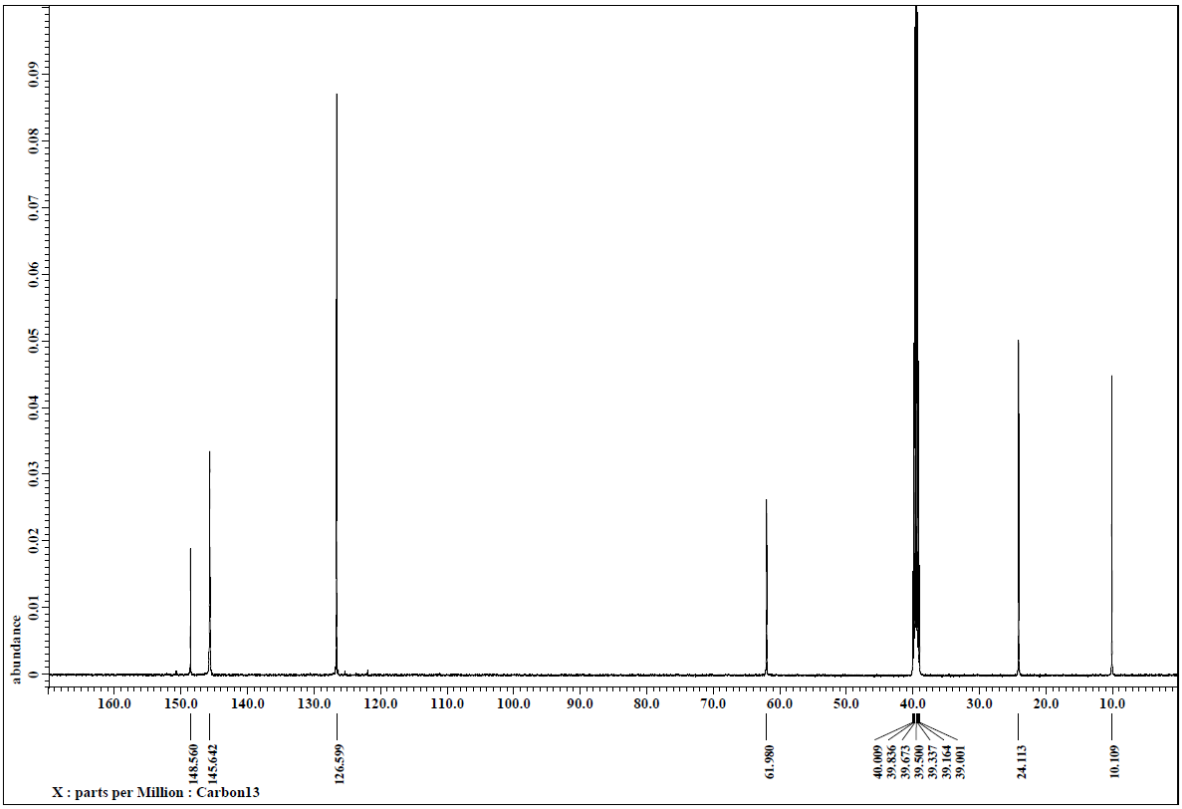

Fig. S1 ^{1}H (top) and ^{13}C NMR (bottom) spectra of **C3^{2+}-2Br^{-}** in DMSO-d_6.

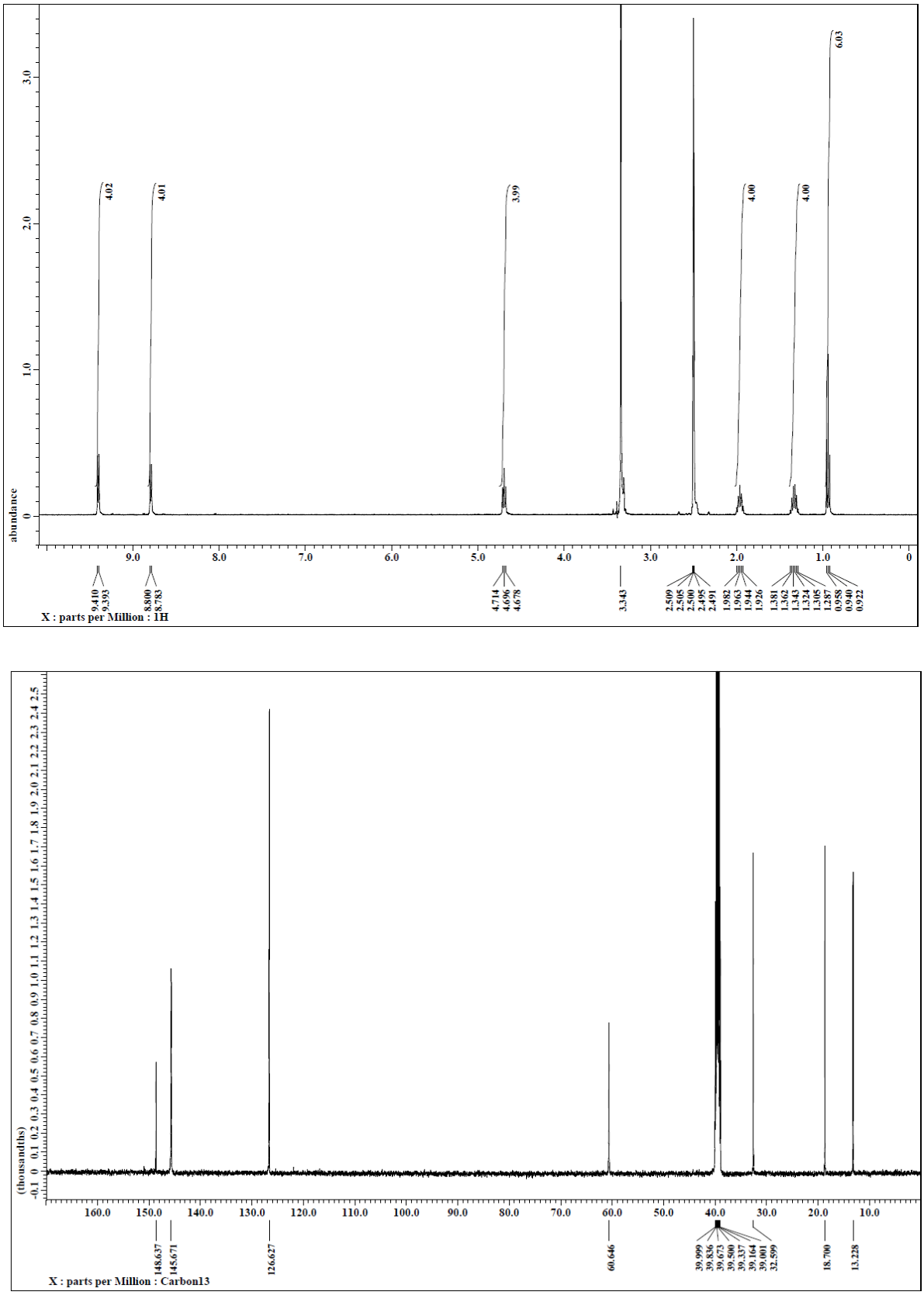

Fig. S2 ^{1}H (top) and ^{13}C NMR (bottom) spectra of **C4^{2+}-2Br^{-}** in DMSO-d_6.

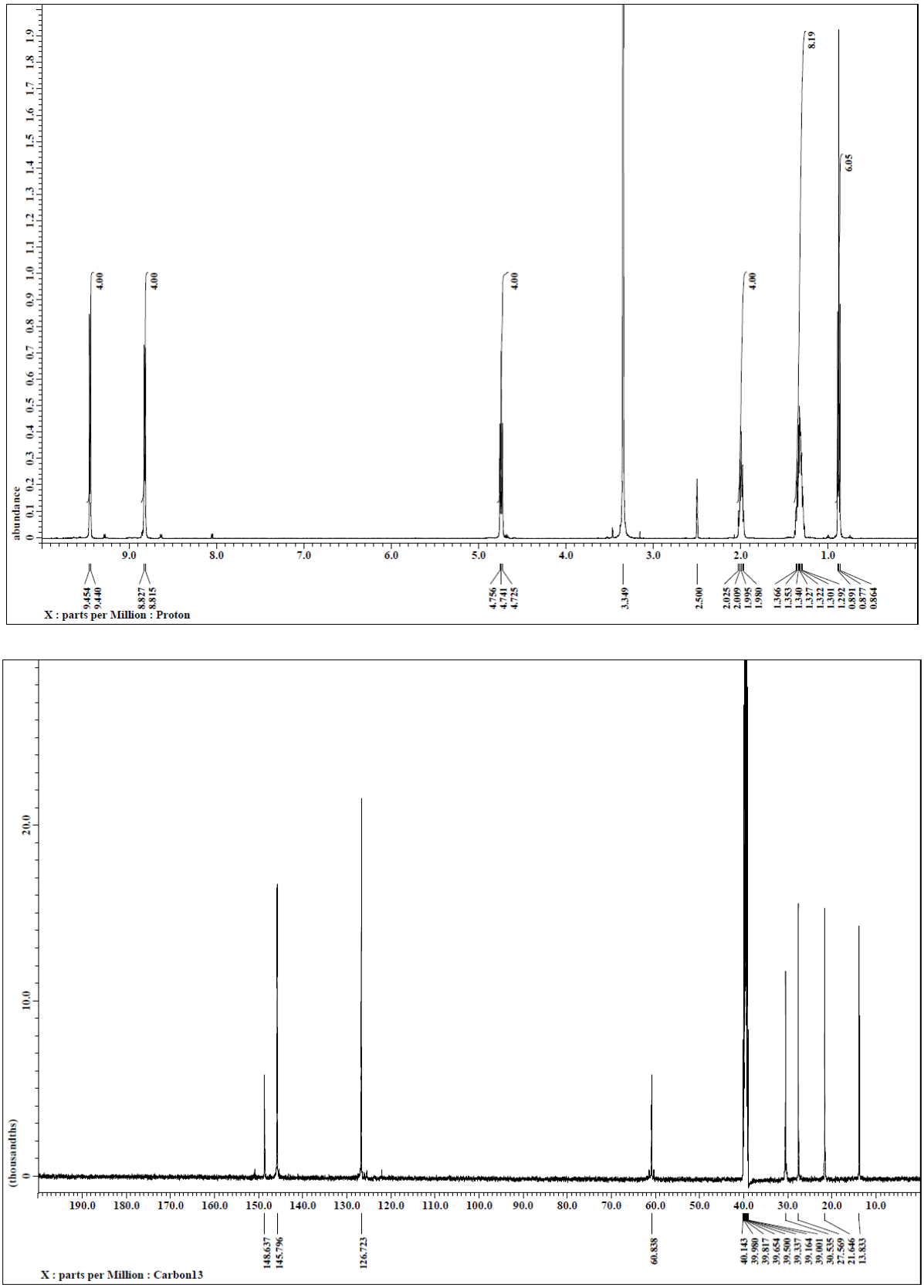

Fig. S3 ^{1}H (top) and ^{13}C NMR (bottom) spectra of **C5^{2+}-2Br^{-}** in DMSO-d_6.

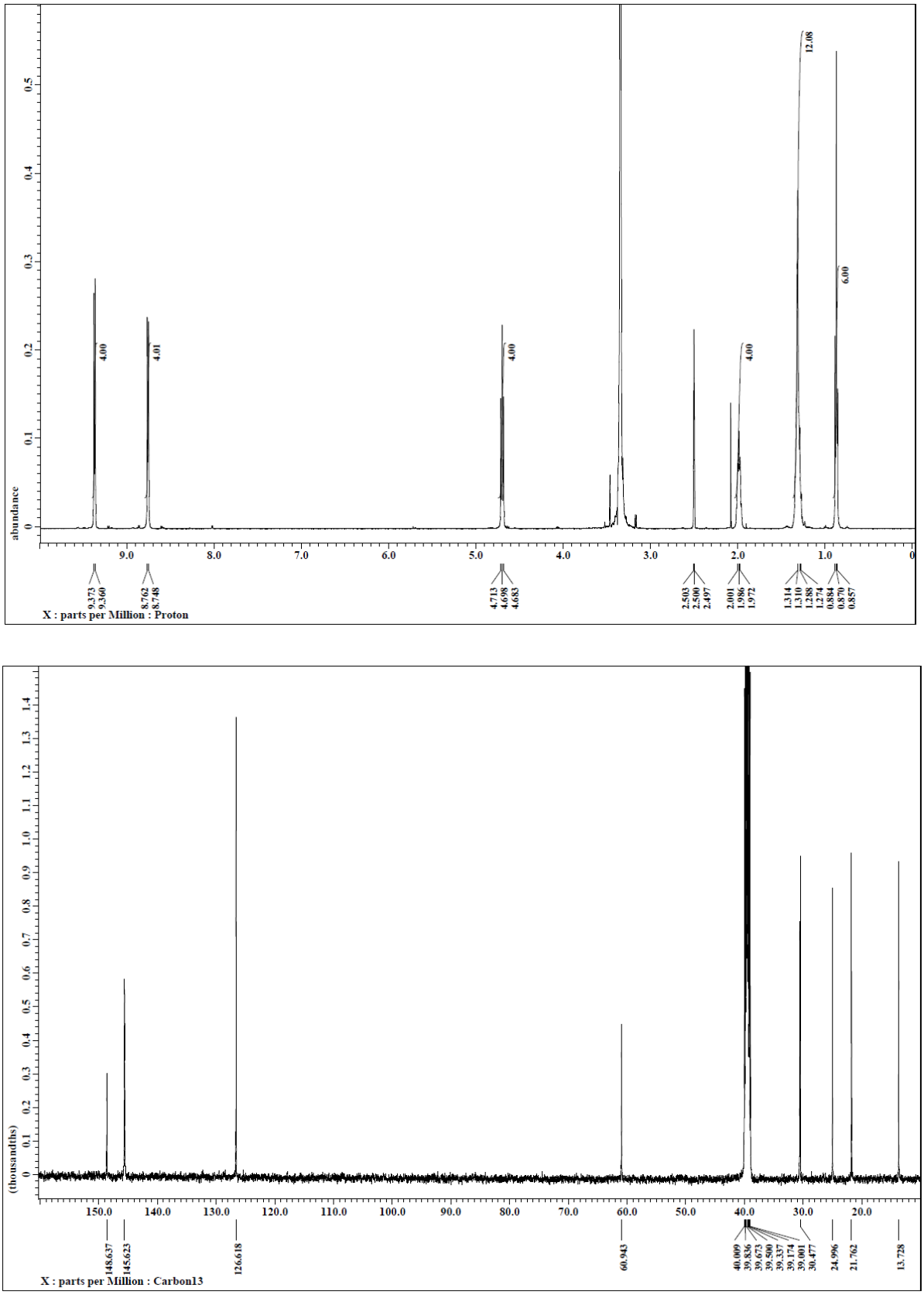

Fig. S4 ^{1}H (top) and ^{13}C NMR (bottom) spectra of **C6^{2+}-2I^{-}** in DMSO-d_6.

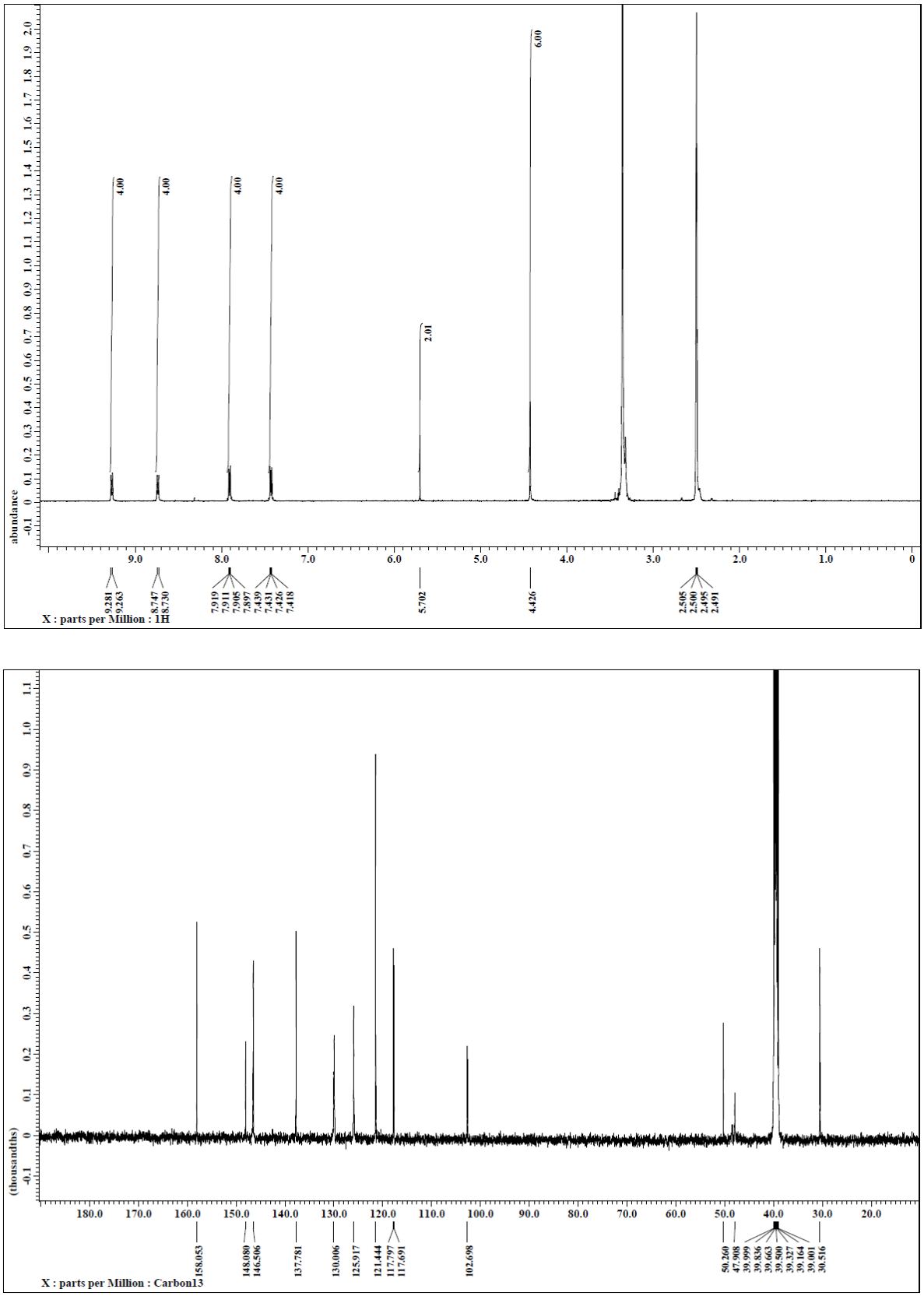

Fig. S5 ^{1}H (top) and ^{13}C NMR (bottom) spectra of **C1^{2+}-2CMI^{-}** in DMSO-d_6.

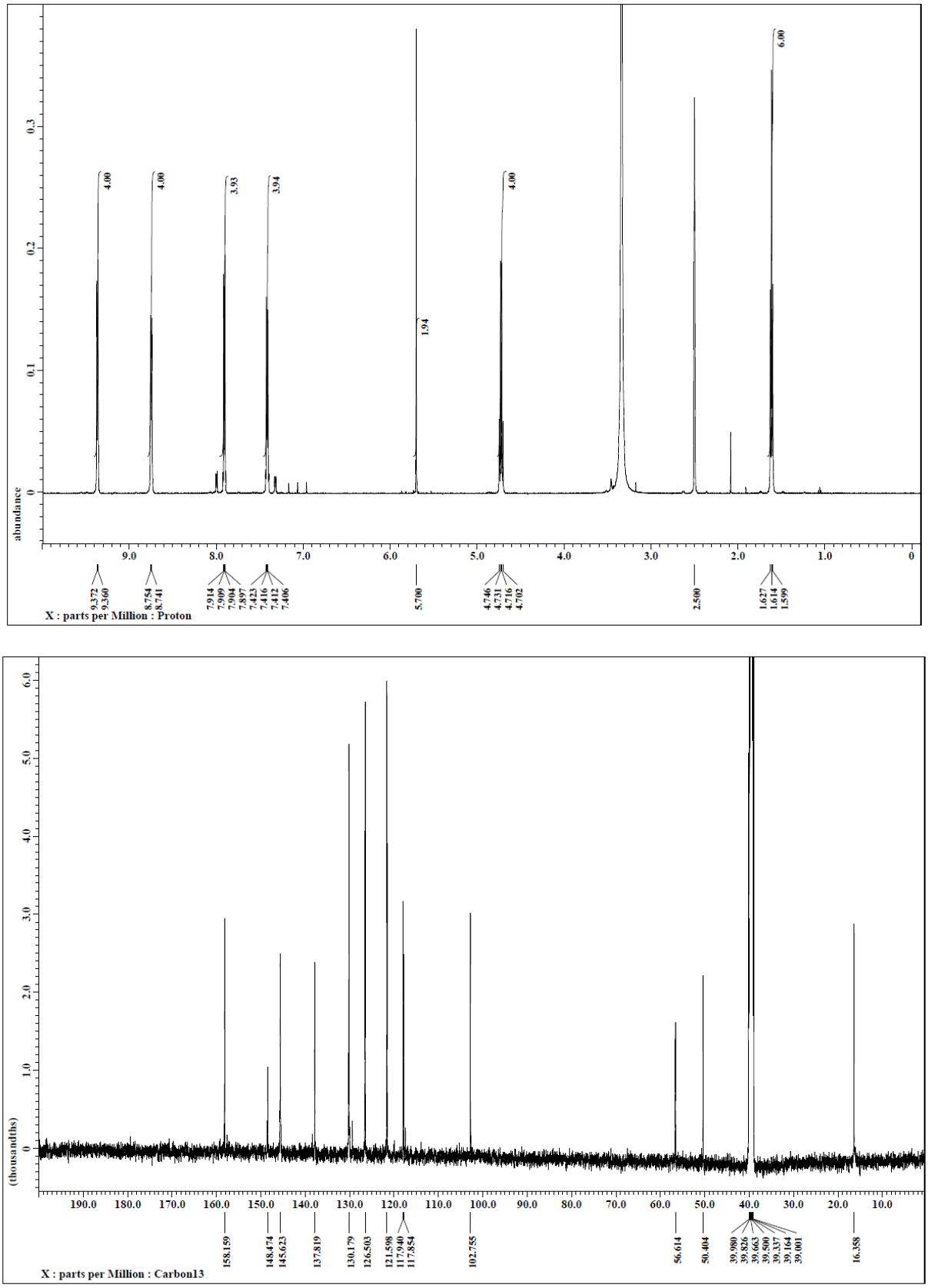

Fig. S6 ^{1}H (top) and ^{13}C NMR (bottom) spectra of **C2^{2+}-2CMI^{-}** in DMSO-d_6.

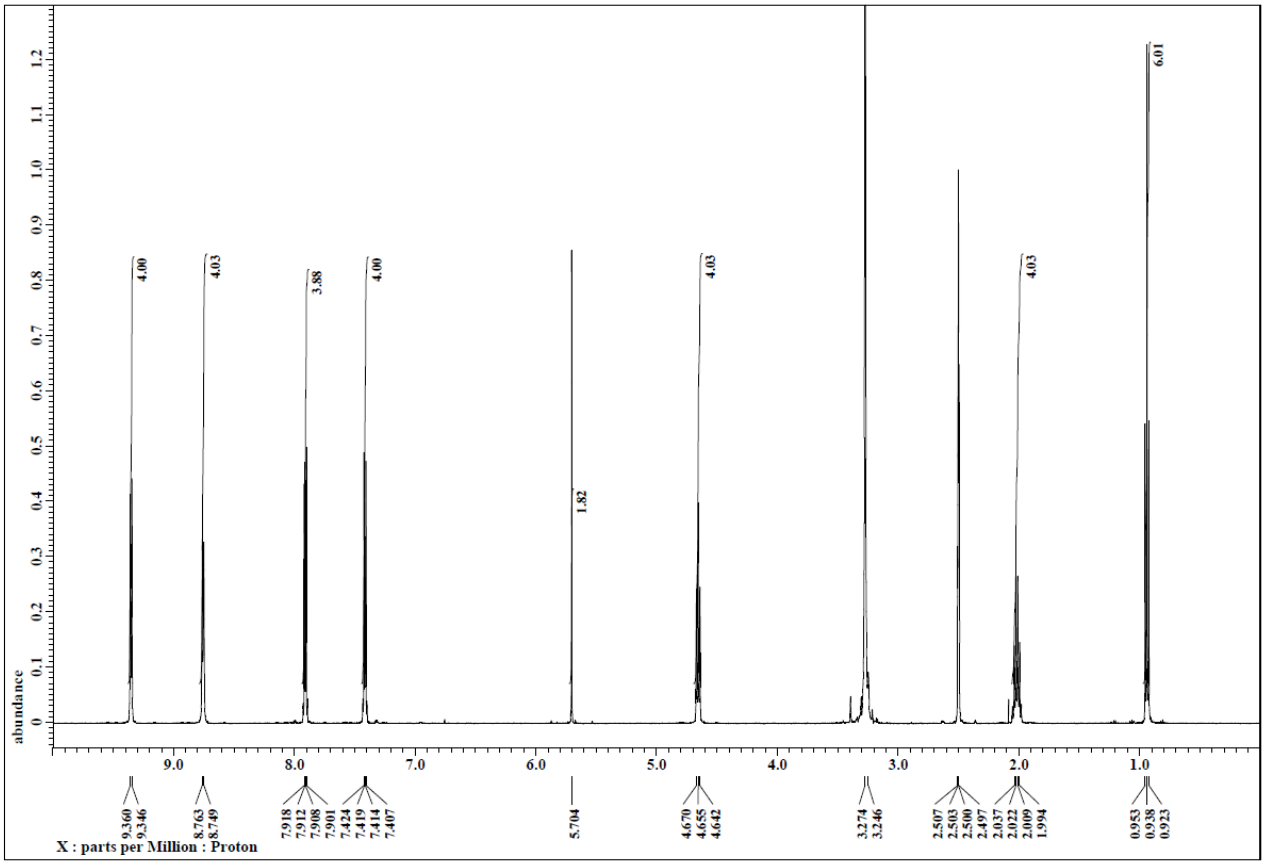

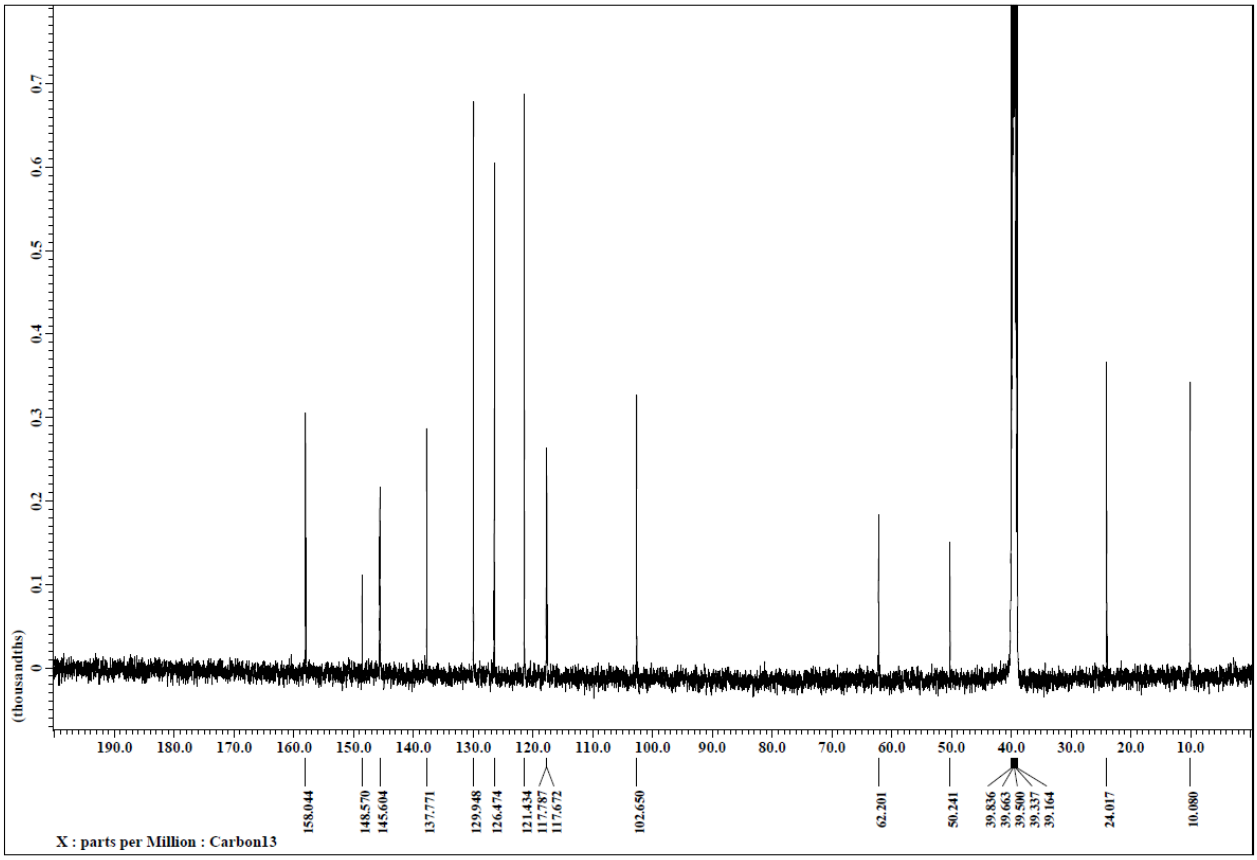

Fig. S7 ^{1}H (top) and ^{13}C NMR (bottom) spectra of **C3^{2+}-2CMI^{-}** in DMSO-d_6.

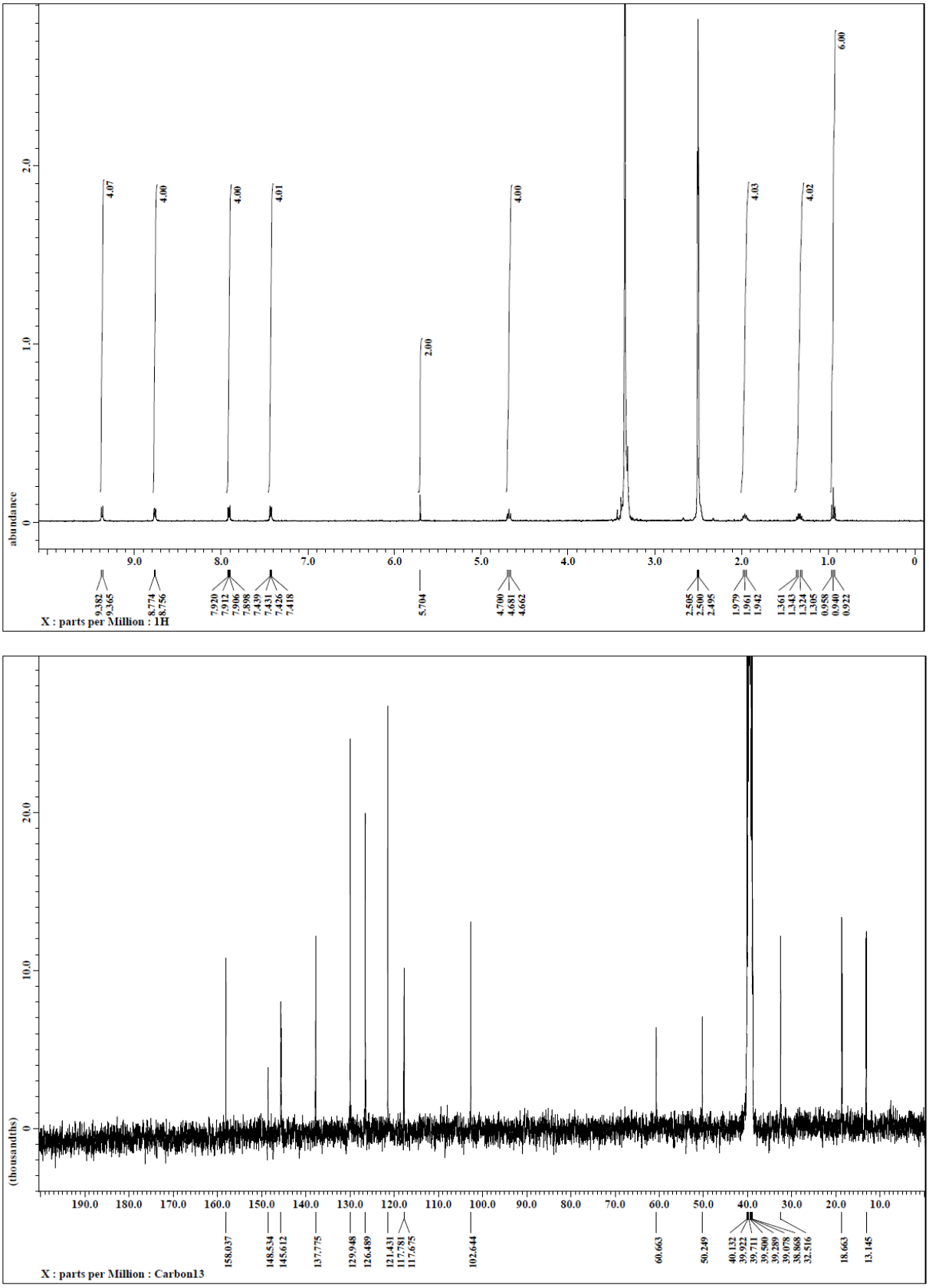

Fig. S8 ^{1}H (top) and ^{13}C NMR (bottom) spectra of **C4^{2+}-2CMI^{-}** in DMSO-d_6.

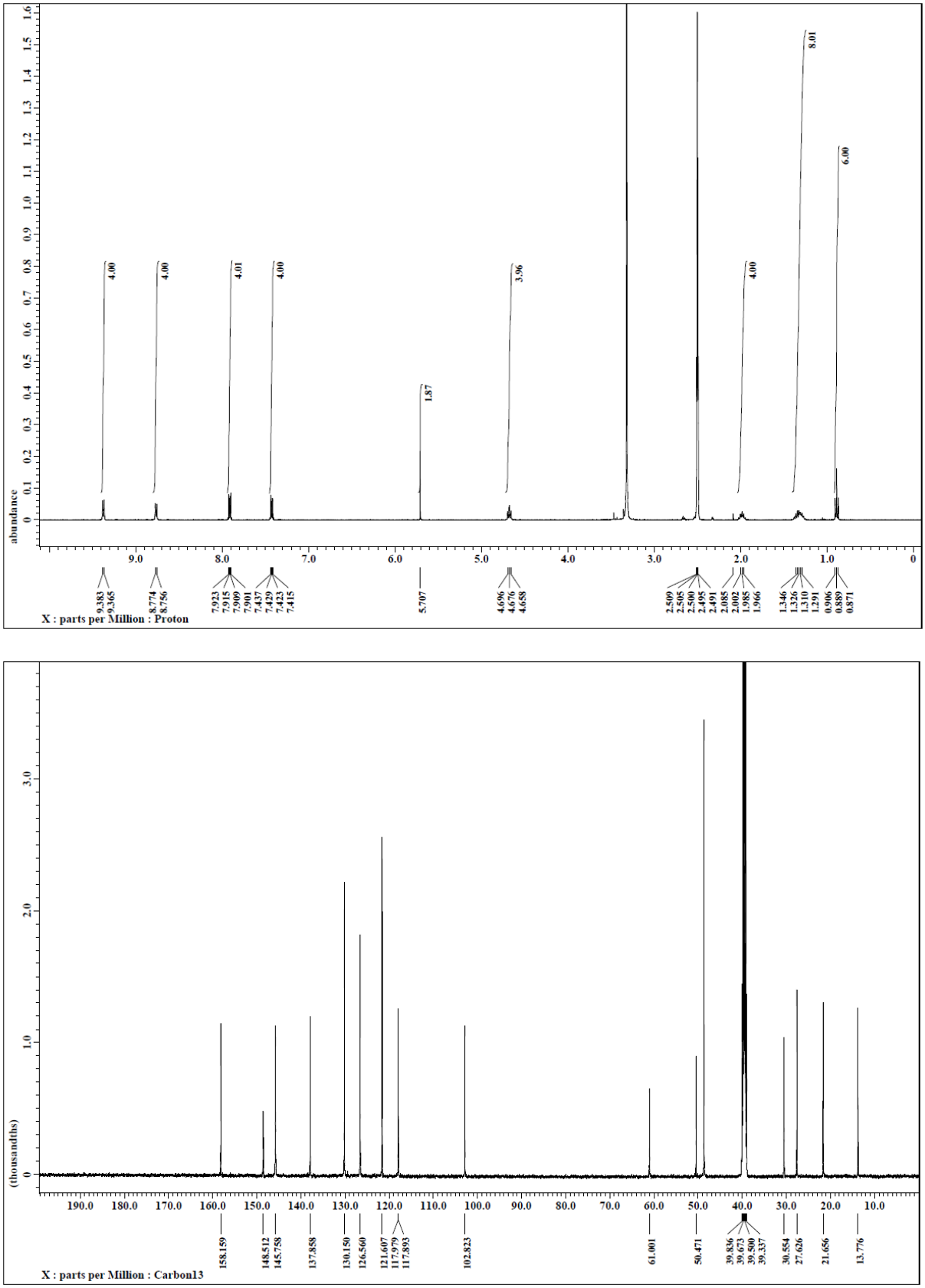

Fig. S9 ^{1}H (top) and ^{13}C NMR (bottom) spectra of **C5^{2+}-2CMI^{-}** in DMSO-d_6.

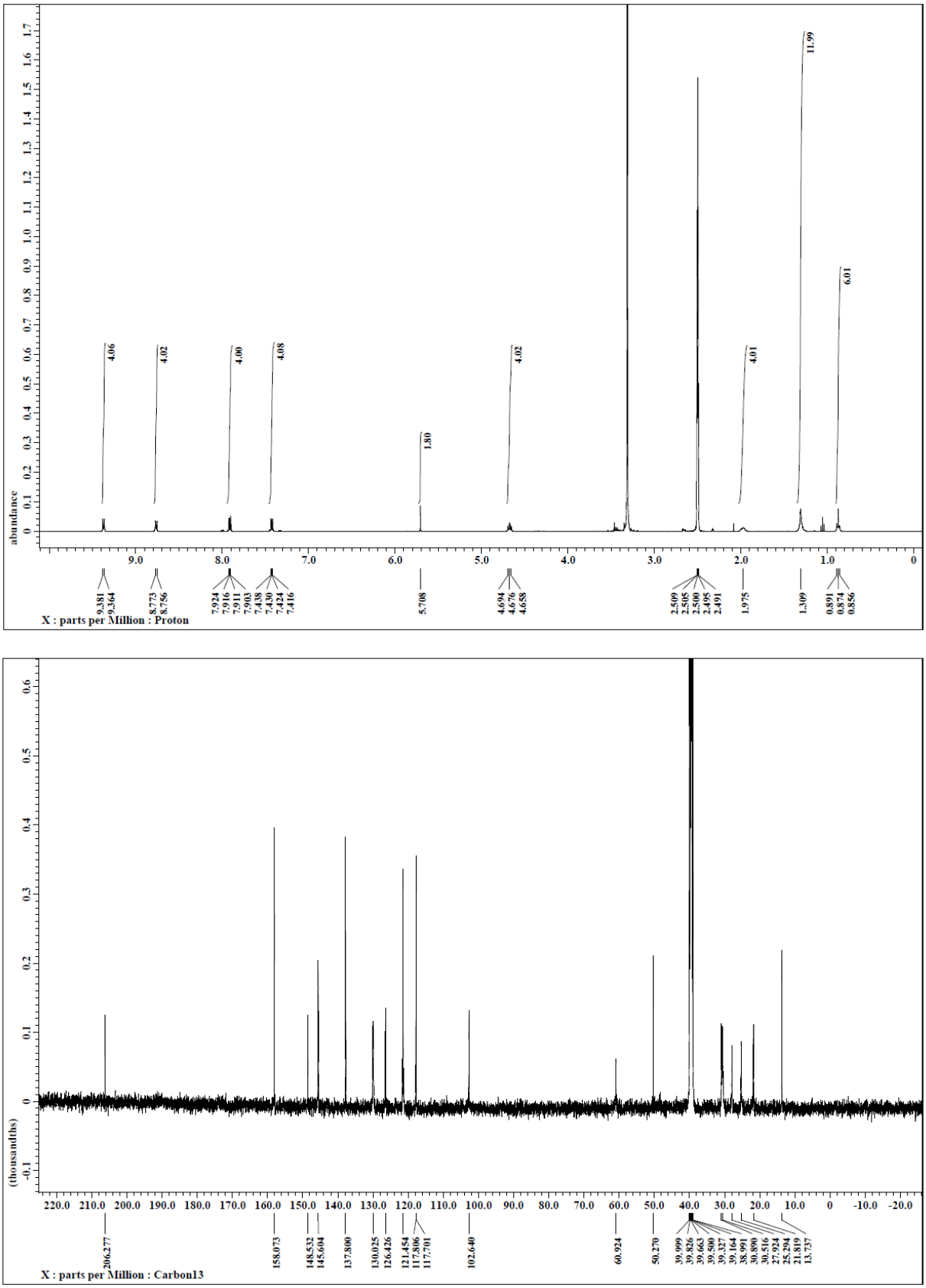

Fig. S10 ^{1}H (top) and ^{13}C NMR (bottom) spectra of **C6^{2+}-2CMI^{-}** in DMSO-d_6.

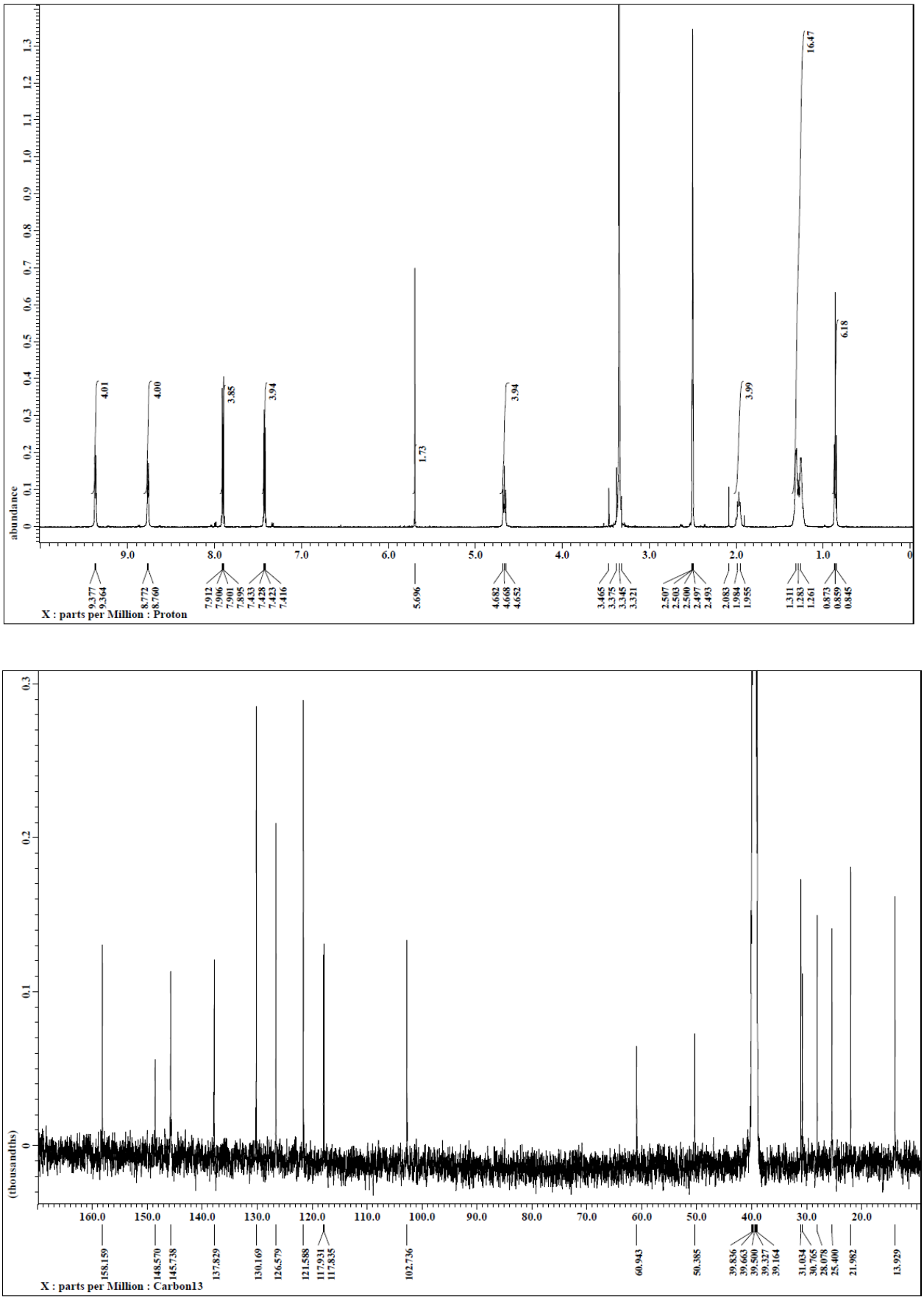

Fig. S11 ^{1}H (top) and ^{13}C NMR (bottom) spectra of **C7^{2+}-2CMI^{-}** in DMSO-d_6.

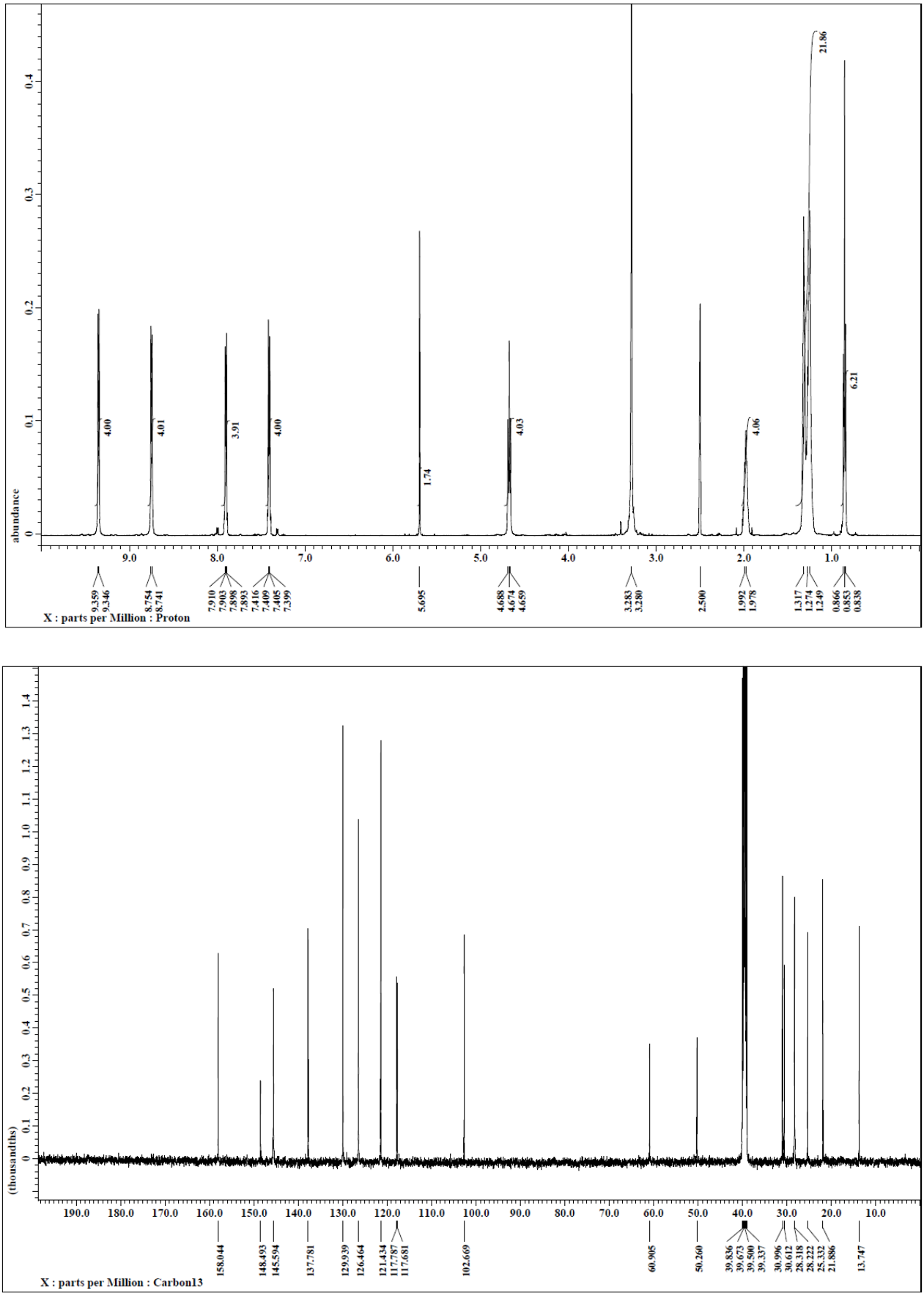

Fig. S12 ^{1}H (top) and ^{13}C NMR (bottom) spectra of **C8^{2+}-2CMI^{-}** in DMSO-d_6.

2. X-ray crystallographic data

X-ray Crystallography. Crystallographic data for the ion pairs of **C1^{2+}-2CMI^{-}**, **C2^{2+}-2CMI^{-}**, **C3^{2+}-2CMI^{-}**, **C4^{2+}-2CMI^{-}**, **C5^{2+}-2CMI^{-}**, and **C6^{2+}-2CMI^{-}** are summarized in Table 1. Single crystals of **C1^{2+}-2CMI^{-}** and **C2^{2+}-2CMI^{-}** were obtained by the slow evaporation of ethanol solutions. Single crystals of **C3^{2+}-2CMI^{-}**, **C4^{2+}-2CMI^{-}**, **C5^{2+}-2CMI^{-}** and **C6^{2+}-2CMI^{-}** were obtained by the vapor diffusion of toluene into the acetone solutions. A single crystal of **C8^{2+}-2CMI^{-}** was obtained by the vapor diffusion of ethyl acetate into the iso-propanol with small quantity of acetone solution. The data for **C1^{2+}-2CMI^{-}**, **C2^{2+}-2CMI^{-}**, **C3^{2+}-2CMI^{-}**, **C4^{2+}-2CMI^{-}**, **C5^{2+}-2CMI^{-}**, and **C6^{2+}-2CMI^{-}** were collected at range of 93 to 150 K on a Rigaku Saturn 724 diffuse reflectance spectra with graphite monochromate Mo-Kα radiation (λ = 0.71073 Å). The data for **C8^{2+}-2CMI^{-}** was collected at 90 K on DECTRIS EIGAR monochromated synchrotron radiation (λ = 0.811069 Å) at BL02B1 (SPring-8). The non-hydrogen atoms were refined anisotropically. In this paper, the π-plane distances out of parallel orientations have been defined as the average lengths between non-hydrogen atoms of π units and the mean planes of their neighboring π units. The CIF files (CCDC-2268733-2268739) can be obtained free of charge from the Cambridge Crystallographic Data Centre via www.ccdc.cam.ac.uk/data_request/cif.

Table S1 Crystallographic details for **C1^{2+}-2CMI^{-}**, **C2^{2+}-2CMI^{-}**, **C3^{2+}-2CMI^{-}**, **C4^{2+}-2CMI^{-}**, **C5^{2+}-2CMI^{-}**, **C6^{2+}-2CMI^{-}**, and **C8^{2+}-2CMI^{-}**.

	C1^{2+}-2CMI^{-}	**C2^{2+}-2CMI^{-}**	**C3^{2+}-2CMI^{-}**	**C4^{2+}-2CMI^{-}**
Formula	$C_{42}H_{24}N_{10}$	$C_{44}H_{28}N_{10}$	$C_{46}H_{32}N_{10}$	$C_{48}H_{36}N_{10}$
fw	334.36	348.38	724.81	752.87
crystal size, mm	0.130 × 0.130 × 0.080	0.200 × 0.150 × 0.100	0.130 × 0.120 × 0.030	0.200 × 0.100 × 0.040
crystal system	Monoclinic	Triclinic	Triclinic	Monoclinic
space group	*C*2/*c* (no. 15)	*P*-1 (no. 2)	*P*-1 (no. 2)	$P2_1/c$ (no. 13)
a, Å	16.3110(4)	8.1502(3)	8.6480(3)	10.8550(2)
b, Å	19.5847(4)	10.8528(3)	11.3059(4)	18.6894(3)
c, Å	11.1122(3)	10.8895(3)	21.0344(7)	10.1304(2)
α, °	90	73.506(2)	74.729(3)	90
β, °	108.012(3)	71.656(3)	82.132(3)	107.219(2)
γ, °	90	89.385(2)	70.001(3)	90
V, Å^3	3375.78(15)	873.35(5)	1861.86(12)	1963.08(6)
ρ_{calcd}, gcm^{-3}	1.316	1.325	1.293	1.274
Z	8	2	2	2
T, K	93	93	150	150
μ, mm^{-1}	0.082 (Mo-Kα)	0.082 (Mo-Kα)	0.080 (Mo-Kα)	0.078 (Mo-Kα)
no. of reflns	27672	11949	21752	25997
no. of unique reflns	3873	3969	6796	4450
variables	241	247	510	266
λ, Å	0.71073 (Mo-Kα)	0.71073 (Mo-Kα)	0.71073 (Mo-Kα)	0.71073 (Mo-Kα)
R_1 ($I > 2\sigma(I)$)	0.0401	0.0426	0.0791	0.0460
wR_2 ($I > 2\sigma(I)$)	0.1058	0.1073	0.1766	0.1280
GOF	1.043	1.033	1.056	1.088
	C5^{2+}-2CMI^{-}	**C6^{2+}-2CMI^{-}**	**C8^{2+}-2CMI^{-}**	
Formula	$C_{50}H_{40}N_{10}$	$C_{52}H_{44}N_{10}$	$C_{59}H_{56}N_{10}O$	
fw	780.92	808.97	921.13	
crystal size, mm	0.160 × 0.140 × 0.040	0.160 × 0.140 × 0.040	0.200 × 0.160 × 0.040	
crystal system	Triclinic	Monoclinic	Triclinic	
space group	*P*-1 (no. 2)	$P2_1/c$ (no. 13)	*P*-1 (no. 2)	
a, Å	11.2406(2)	8.25330(10)	9.5662(2)	
b, Å	13.7520(3)	16.1442(3)	12.9105(3)	
c, Å	14.5481(3)	17.4065(4)	13.0276(3)	
α, °	68.229(2)	90	64.830(2)	
β, °	75.915(2)	110.275(2)	87.544(2)	
γ, °	85.545(2)	90	69.361(2)	
V, Å^3	2025.47(8)	2175.59(7)	1351.81(6)	
ρ_{calcd}, gcm^{-3}	1.28	1.235	1.132	
Z	2	2	1	
T, K	150	150	293	
μ, mm^{-1}	0.079 (Mo-Kα)	0.076 (Mo-Kα)	0.070 (synchrotron)	
no. of reflns	28031	29170	71607	
no. of unique reflns	9221	4952	13259	
variables	549	284	338	
λ, Å	0.71073 (Mo-Kα)	0.71073 (Mo-Kα)	0.81107 (synchrotron)	
R_1 ($I > 2\sigma(I)$)	0.0637	0.0423	0.0618	
wR_2 ($I > 2\sigma(I)$)	0.1632	0.1108	0.1903	
GOF	1.056	1.027	1.038	

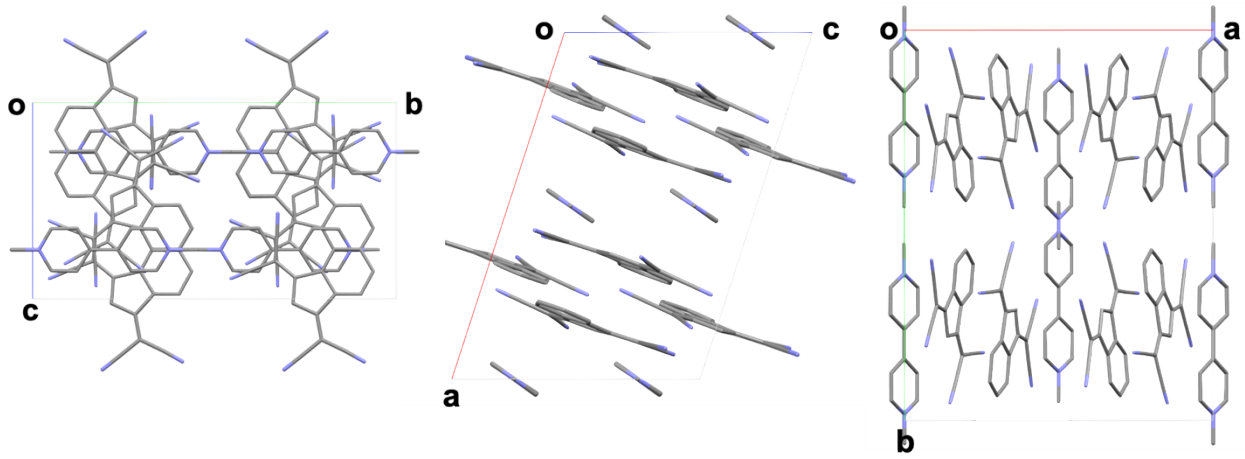

Fig. S13 Packing diagrams (viewed along the *a*, *b*, and *c* axes) of **C1**$^{2+}$**-2CMI**$^{-}$.

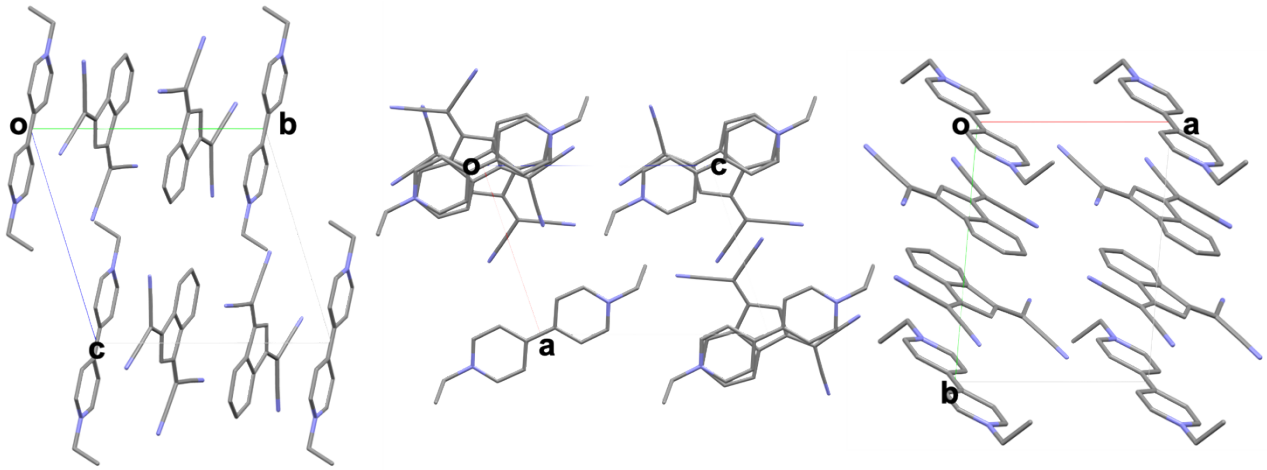

Fig. S14 Packing diagrams (viewed along the *a*, *b*, and *c* axes) of **C2**$^{2+}$**-2CMI**$^{-}$.

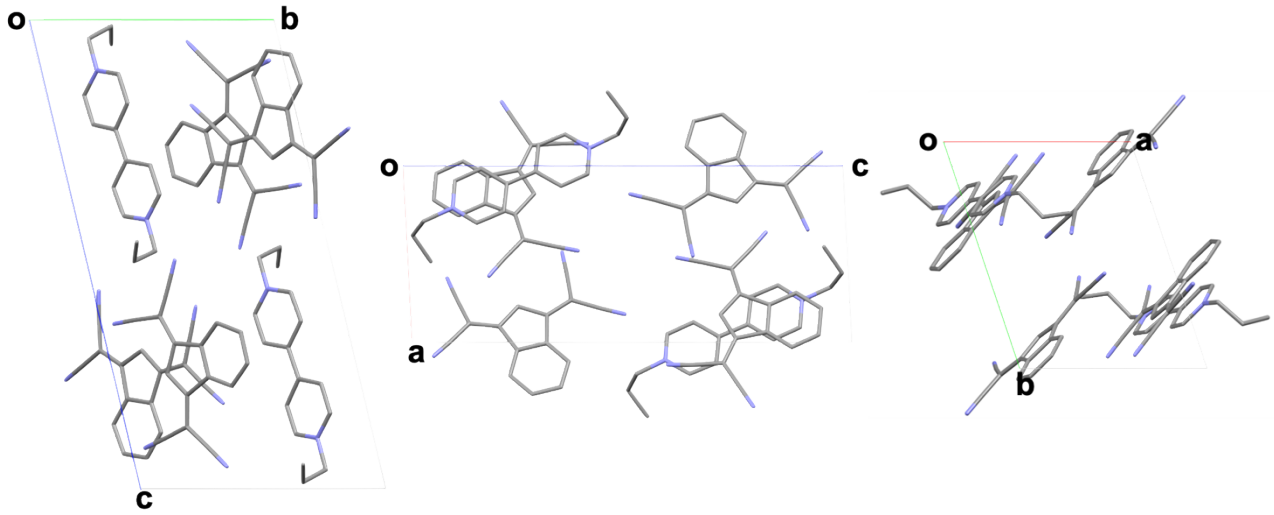

Fig. S15 Packing diagrams (viewed along the *a*, *b*, and *c* axes) of **C3**$^{2+}$**-2CMI**$^{-}$.

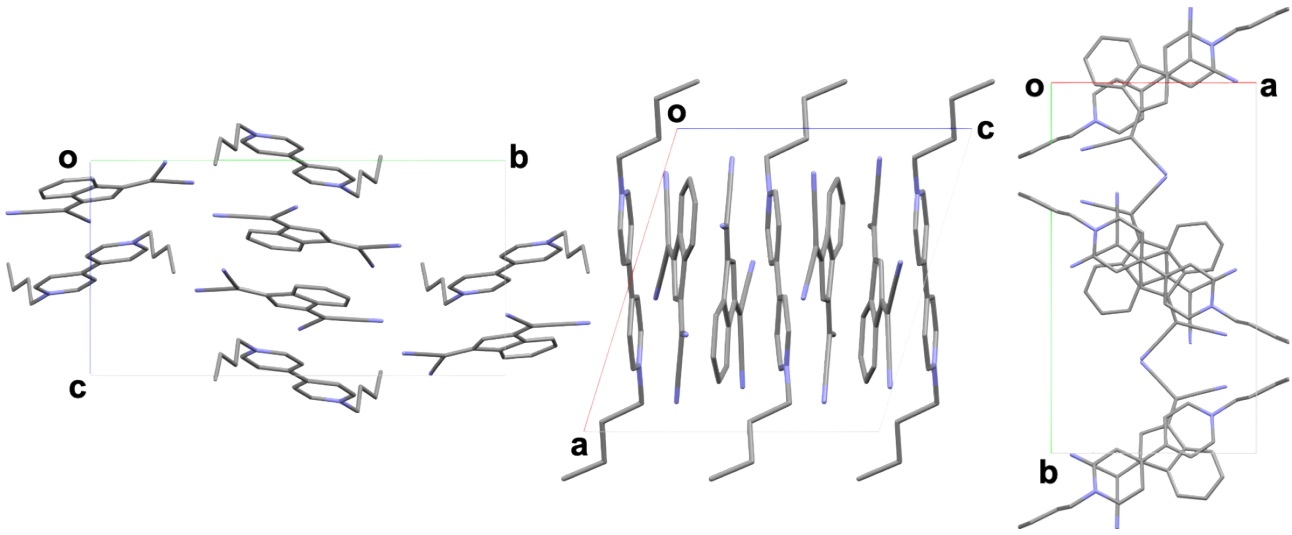

Fig. S16 Packing diagrams (viewed along the *a*, *b*, and *c* axes) of **C4^{2+}-2CMI^{-}**.

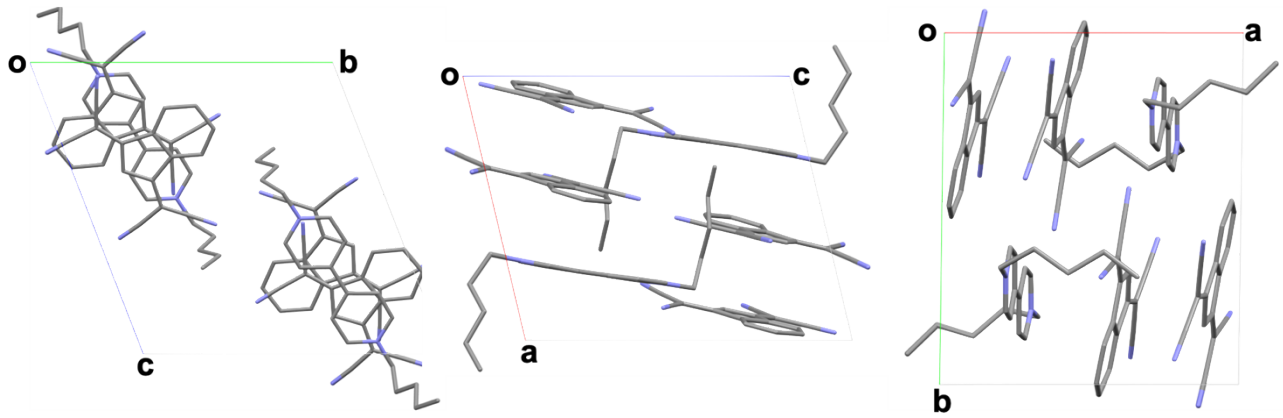

Fig. S17 Packing diagrams (viewed along the *a*, *b*, and *c* axes) of **C5^{2+}-2CMI^{-}**.

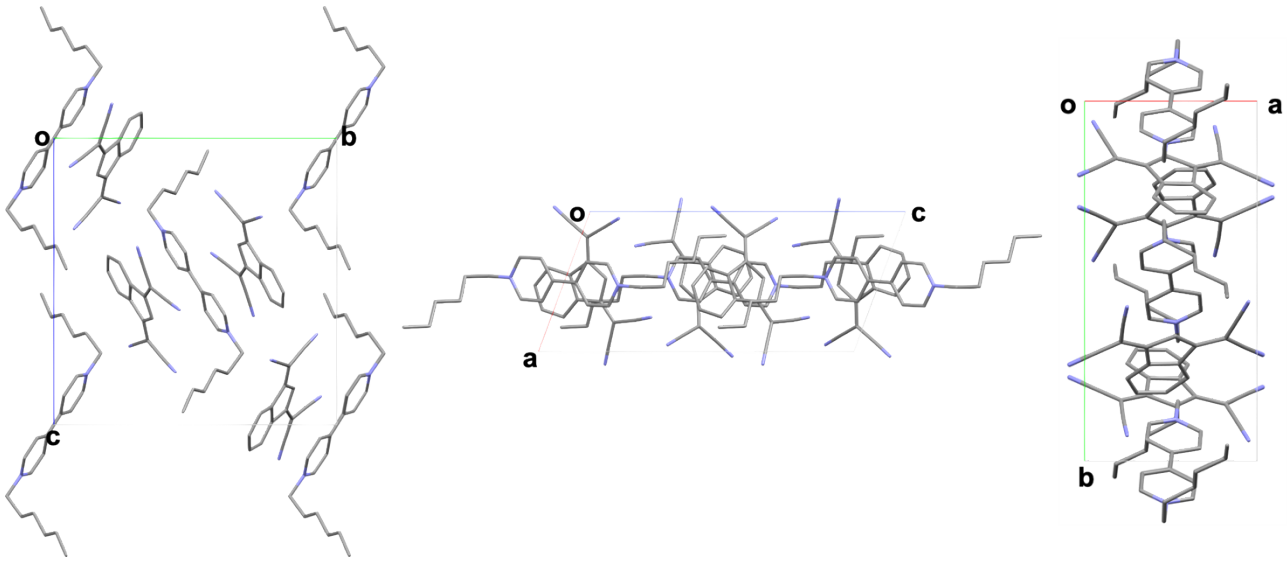

Fig. S18 Packing diagrams (viewed along the *a*, *b*, and *c* axes) of **C6^{2+}-2CMI^{-}**.

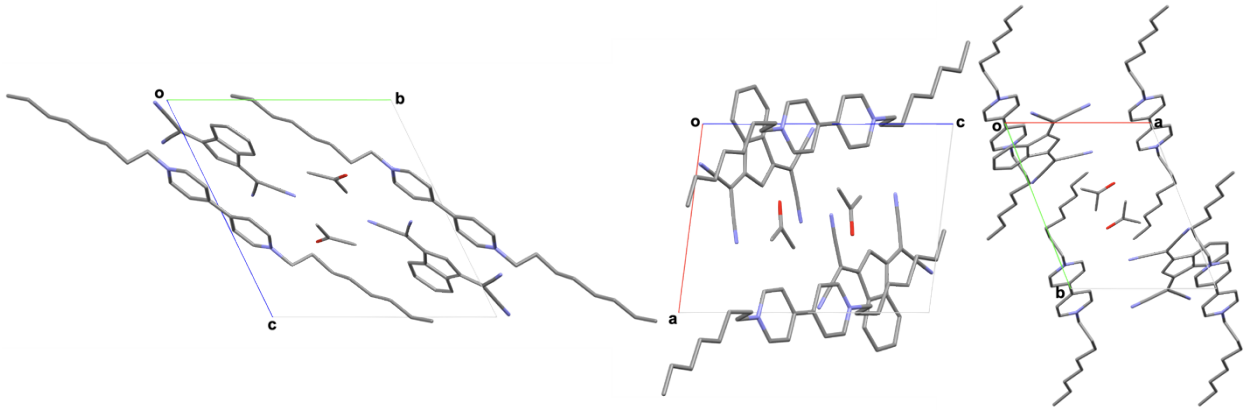

Fig. S19 Packing diagrams (viewed along the *a*, *b*, and *c* axes) of **C8^{2+}-2CMI^{-}**.

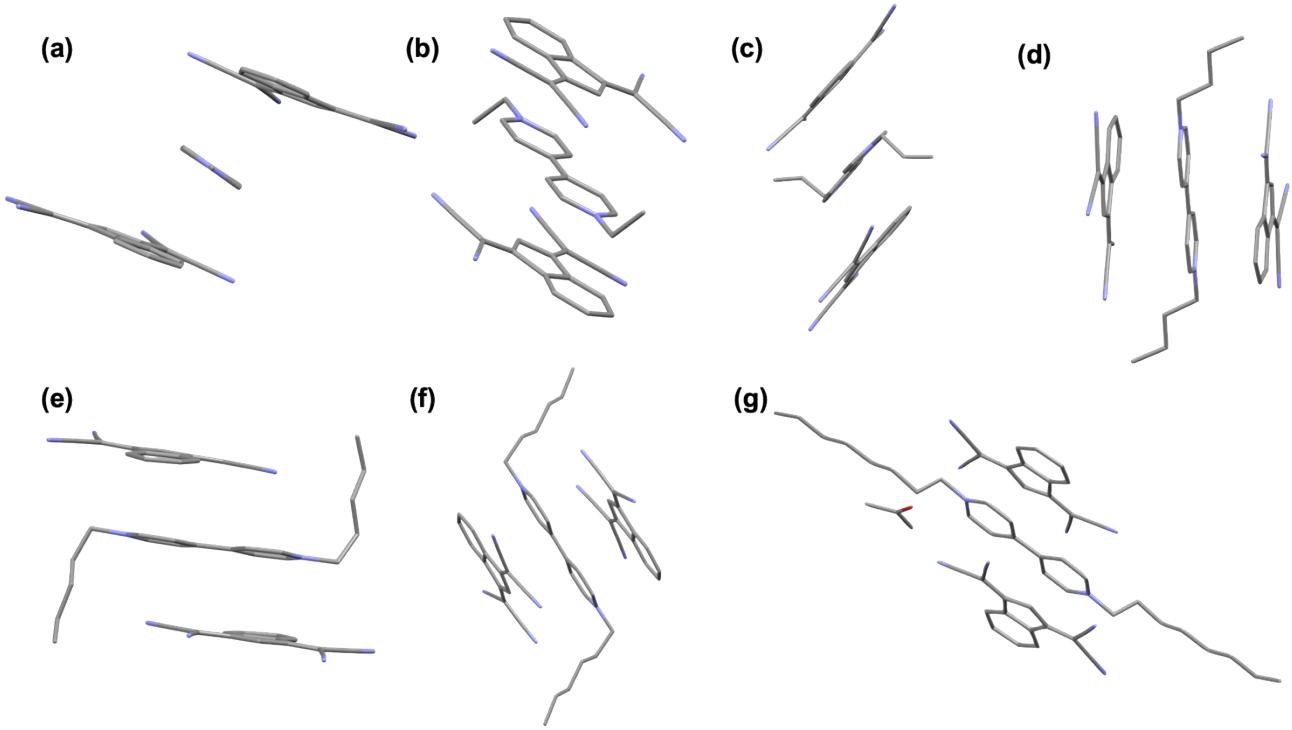

Fig. S20 Summarize of the stacking formation (D-A-D) of ion pairs in (a) **C1^{2+}-2CMI^{-}**, (b) **C2^{2+}-2CMI^{-}**, (c) **C3^{2+}-2CMI^{-}**, (d) **C4^{2+}-2CMI^{-}**, (e) **C5^{2+}-2CMI^{-}**, (f) **C6^{2+}-2CMI^{-}** and (g) **C8^{2+}-2CMI^{-}**.

3. Optical properties

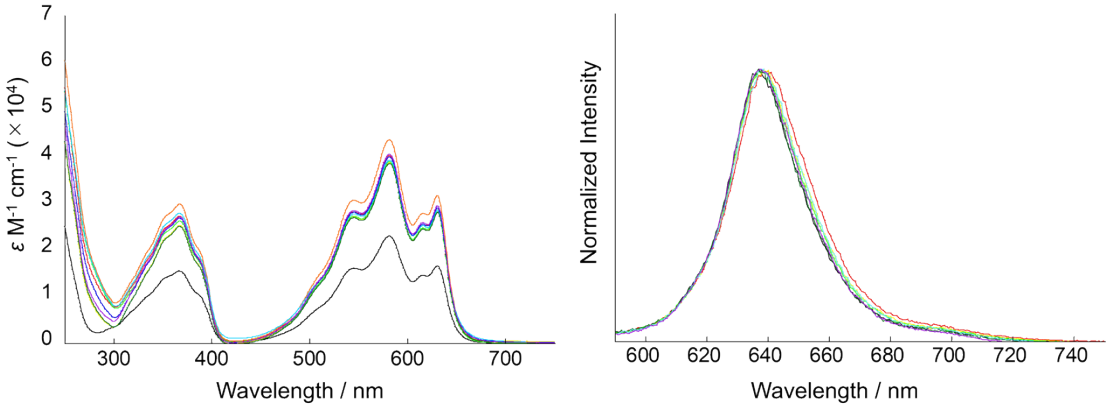

Fig. S21 (a) UV/vis absorption and (b) fluorescence spectra (10^{-5} M in MeOH) of **Na^{+}-CMI^{-}** (black), **C1^{2+}-2CMI^{-}** (red), **C2^{2+}-2CMI^{-}** (orange), **C3^{2+}-2CMI^{-}** (yellow), **C4^{2+}-2CMI^{-}** (light green), **C5^{2+}-2CMI^{-}** (green), **C6^{2+}-2CMI^{-}** (blue), **C7^{2+}-2CMI^{-}** (purple) and **C8^{2+}-2CMI^{-}** (purple). The fluorescence spectra were obtained by excitation at the respective absorption maxima.

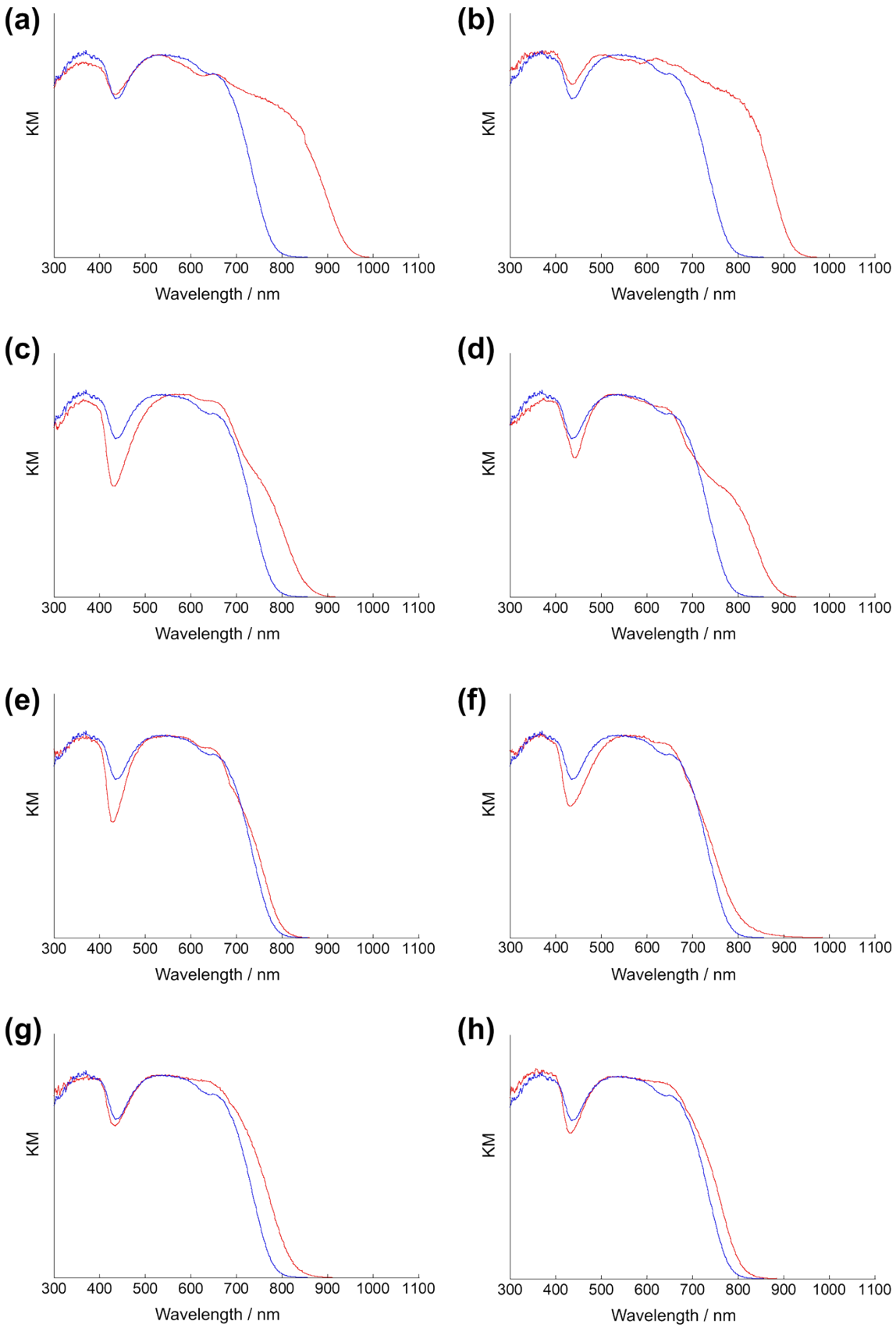

Fig. S22 Diffuse reflectance spectra of (a) **C1^{2+}-2CMI^{-}**, (b) **C2^{2+}-2CMI^{-}**, (c) **C3^{2+}-2CMI^{-}**, (d) **C4^{2+}-2CMI^{-}**, (e) **C5^{2+}-2CMI^{-}**, (f) **C6^{2+}-2CMI^{-}**, (g) **C7^{2+}-2CMI^{-}** and (h) **C8^{2+}-2CMI^{-}** shown in red lines compared with Na^{+}-**CMI^{-}** shown in blue line. Notably, **Cn^{2+}-2CMI^{-}** (n = 1–4) showed a remarkably divergent wavelength of absorption edge compared to Na^{+}-**CMI^{-}**. Their absorption are extended towards near-infrared, demonstrating a charge-transfer character.

4. Thermal properties

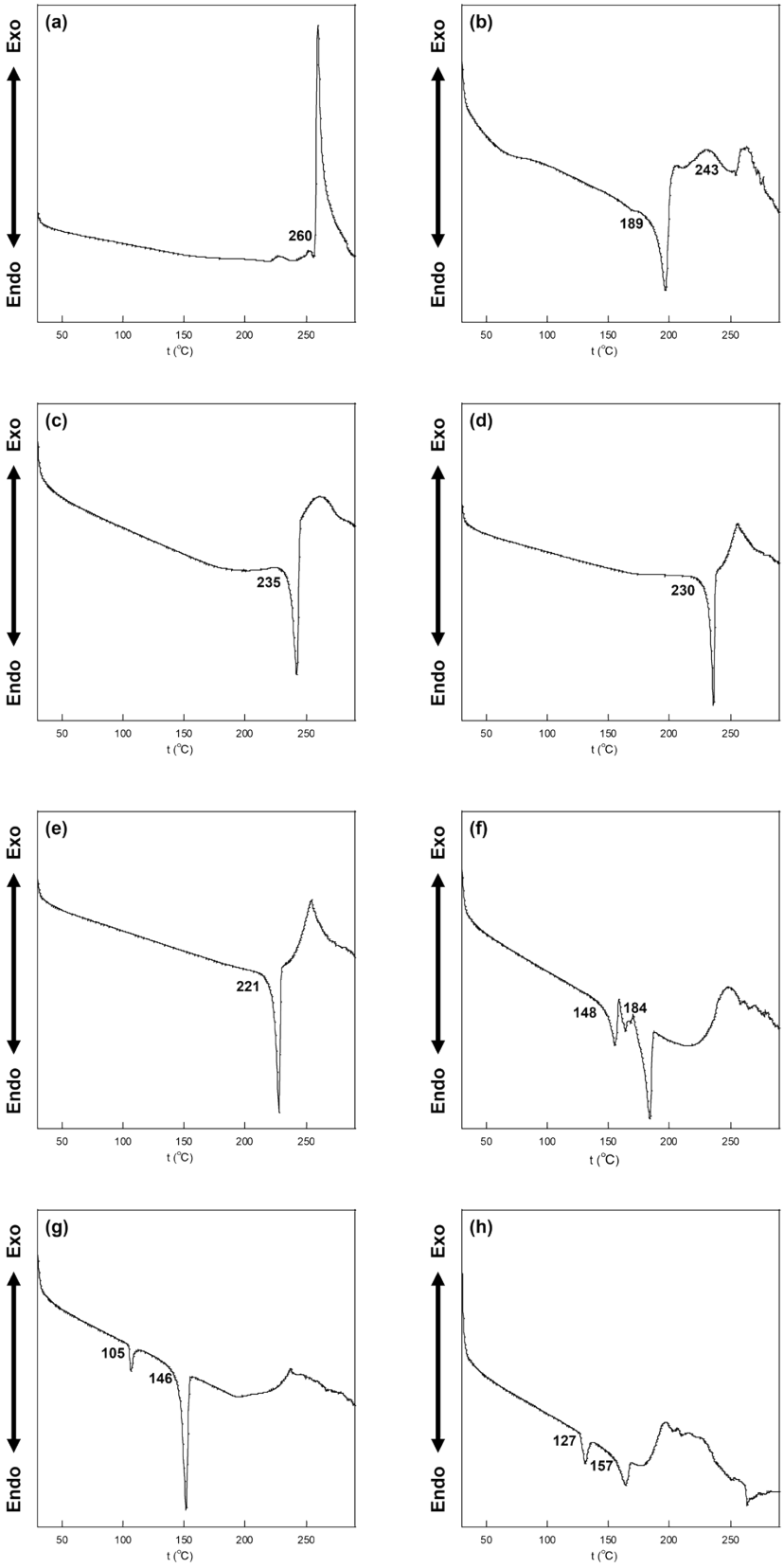

Fig. S23 DSC thermograms of (a) **C1^{2+}-2CMI^{-}**, (b) **C2^{2+}-2CMI^{-}**, (c) **C3^{2+}-2CMI^{-}**, (d) **C4^{2+}-2CMI^{-}**, (e) **C5^{2+}-2CMI^{-}**, (f) **C6^{2+}-2CMI^{-}**, (g) **C7^{2+}-2CMI^{-}** and (h) **C8^{2+}-2CMI^{-}**. Onset temperatures (°C) of melting points are labeled. **C1^{2+}-2CMI^{-}** showed an exothermic peak at 260°C, indicating its decomposition before melting.